

New limits on warm inflation from pulsar timing arrays

Rocco D'Agostino^{1,2,*} and Matteo Califano^{1,2,†}

¹*Scuola Superiore Meridionale, Largo San Marcellino 10, 80138 Napoli, Italy*

²*Istituto Nazionale di Fisica Nucleare (INFN), Sezione di Napoli, Via Cinthia 21, 80126 Napoli, Italy*

In this paper, we investigate scalar-induced gravitational waves (GWs) generated in the post-inflationary universe to infer new limits on warm inflation. We specifically examine the evolution of primordial GWs produced by scalar perturbations produced during the radiation-dominated epoch. For this purpose, we assume a weak regime of warm inflation under the slow-roll approximation, with a dissipation coefficient linearly dependent on the temperature of the radiation bath. We then derive analytical expressions for the curvature power spectrum and the scalar index, in the cases of chaotic and exponential potentials of the inflationary field. Subsequently, we compare the theoretical predictions regarding the relic energy density of GWs with the stochastic GW background signal recently detected by the NANOGrav collaboration through the use of pulsar timing array measurements. In so doing, we obtain numerical constraints on the free parameters of the inflationary models under study. Finally, we conduct a model selection analysis through the Bayesian inference method to measure the statistical performance of the different theoretical scenarios.

I. INTRODUCTION

Cosmic inflation stands as the most widely accepted theory for addressing the puzzles of homogeneity, flatness, and the monopole problem within the framework of the hot Big Bang model [1–4]. Additionally, the inflationary mechanism serves as the foundation for the initial seeds of all large structures in the universe. The standard inflationary paradigm is strictly connected to a dynamical scalar field, known as the *inflaton*, which rolls down its potential during the exponential expansion of the very early universe. During inflation, the motion of this field is slowed down due to the coupling with the background spacetime. At the end of inflation, the universe is left in a highly cooled state due to the absence of radiation production during the inflationary era, as a result of the non-interaction of the inflaton with other fields. Therefore, the issue of the transition from inflation to the radiation-dominated epoch is referred as to the *graceful exit* problem. The first solution to the latter was achieved by considering, right after inflation, a reheating phase during which couplings with other fields would result in an oscillatory behavior of the inflaton field, giving rise to particle production [5–7].

Among the several alternatives to the original cold inflation picture, the warm inflation scenario is perhaps one of the most attractive [8–14]. Warm inflation represents an attempt to provide consistent inflationary dynamics from a quantum field theory perspective. In this case, the graceful exit problem is solved by the presence of radiation during inflation, allowing for a smooth transition to the radiation-dominated era without the need for a distinct reheating phase. Contrary to the standard cold inflation picture, in the warm inflation scenario, the presence of interactions between the inflaton and other fields

during the inflationary phase leads to dissipation effects and fluctuations. Eventually, the vacuum energy of the inflaton is released to the other fields resulting in particle production that contributes to the next radiation-dominated epoch [15].

The quantum field theory realization of warm inflation was investigated in Refs. [16–18], where the dissipation effects and fluctuations were linked to the overdamped evolution of the inflaton field. Such overdamped behavior is expected to take place in an adiabatic regime where microscopic phenomena happen much faster compared to the Hubble expansion and the evolution of the inflaton. An effective challenge in constructing warm inflation models lies in dealing with thermal and quantum corrections to the inflaton that could produce strong deviations from a flat potential and, hence, inhibit inflation itself. To circumvent this issue, supersymmetric approaches and the introduction of couplings between the inflaton and heavy intermediate fields were considered in the earlier works [15, 19]. Also, more recent analyses have shown that corrections to the inflaton potential can be efficiently regulated by relying only on symmetry properties [20–22].

Typically, maintaining a nearly thermal bath during warm inflation is possible under significant dissipation. This dissipation should be strong enough to enable the conversion of a portion of the energy stored in the inflaton into radiation. Strong dissipation regimes of warm inflation have demonstrated potentially appealing within the context of effective field theory [23–25]. On the other hand, in the weak regime of warm inflation, where the dissipation effects are sub-dominant in the evolution of the inflaton field during inflation, thermal fluctuations constitute the predominant contributor to the creation of the initial perturbations, and the resulting thermal bath proves sufficient to warm up the universe after the inflationary phase [26, 27]. Moreover, the weak dissipation scenario provides a natural explanation to a major challenge of quintessential inflation models, in which the inflaton field survives until the present day and cannot

* rocco.dagostino@unina.it

† matteo.califano@unina.it

account for the reheating process [28].

A comprehensive review of the latest advancements in warm inflation is available in Ref. [29], where several applications of dissipative dynamics are discussed to address some of the cosmological issues typical of cold inflation. More recently, warm inflation has been revisited in Ref. [30] through a numerical Fokker-Planck approach to test monomial potentials with current CMB bounds.

The current era of gravitational wave (GW) astronomy has provided us with novel tools for investigating cosmology and fundamental physics [31–41]. In this respect, a crucial role is played by primordial scalar perturbations, acting as a source for second-order tensor fluctuations. These scalar-induced GWs are generated when the primordial perturbations re-enter the horizon in the post-inflationary era, offering unique insights into the final stages of inflation and encoding valuable information about the composition of the early universe [42–45]. In particular, scalar-induced GWs have been considered as a potential cosmological interpretation of the GW background signal observed by the NANOGrav collaboration through the use of pulsar timing array (PTA) measurements [46–51]. Here, we examine the implications of such observations on the curvature power spectrum of scalar-induced GWs within the framework of warm inflation.

This paper is organized as follows. In Sec. II, we recall the fundamentals of the warm inflation background dynamics and perturbations, emphasizing the main differences with respect to the standard cold inflation scenario. In Sec. III, we explore the propagation of scalar-induced GWs during the radiation-dominated epoch, as well as the associated relic energy density. In Sec. IV, we obtain the shape of the primordial curvature power spectrum for two classes of inflationary potentials, namely chaotic and exponential models, under the weak dissipation regime of warm inflation. In Sec. V, we test our models through the most recent release of NANOGrav data of PTAs. Additionally, we compare our results with the predictions of the cosmic microwave background (CMB) anisotropies. Finally, in Sec. VI, we summarize our findings and outline the possible future perspectives of our work.

Throughout this study, we adopt units of $c = \hbar = 1$, and denote the reduced Planck mass as $M_P \equiv 1/\sqrt{8\pi G}$.

II. WARM INFLATION SCENARIO

We consider the spatially flat Friedmann-Lemaître-Robertson-Walker metric

$$ds^2 = -dt^2 + a(t)^2 \delta_{ij} dx^i dx^j, \quad (1)$$

where $a(t)$ is the scale factor as a function of cosmic time, t . The background dynamics in the warm inflation scenario is described by the first Friedmann equation

$$H^2 = \frac{1}{3M_P^2}(\rho_r + \rho_\phi), \quad (2)$$

where $H \equiv \frac{\dot{a}}{a}$ is the Hubble parameter, while ρ_r and ρ_ϕ are the energy density of radiation and the inflationary field, respectively. The evolution of the cosmic fluid is given by the following system [52]:

$$\dot{\rho}_r + 3H(\rho_r + p_r) = \Gamma(\rho_\phi + p_\phi), \quad (3)$$

$$\dot{\rho}_\phi + 3H(\rho_\phi + p_\phi) = -\Gamma(\rho_\phi + p_\phi), \quad (4)$$

where the dot indicates the derivative with respect to t , and $\Gamma(\phi, T)$ is the dissipation coefficient, which can generally depend on the inflaton field and the temperature of the radiation bath, T . Moreover, $p_r = \frac{\rho_r}{3}$ is the radiation pressure, where $\rho_r = \frac{\pi^2}{30} g_{\text{eff}} T^4$, with g_{eff} being the effective degrees of freedom of relativistic species and T is the temperature of the radiation bath. Also, for a canonical inflationary field, we have $\rho_\phi = \frac{\dot{\phi}^2}{2} + V(\phi)$ and $p_\phi = \frac{\dot{\phi}^2}{2} - V(\phi)$, where $V(\phi)$ is the inflaton potential. Hence, Eqs. (3) and (4) take the form

$$\dot{\rho}_r + 4H\rho_r = \Gamma\dot{\phi}^2, \quad (5)$$

$$\ddot{\phi} + (3H + \Gamma)\dot{\phi} + V_{,\phi} = 0, \quad (6)$$

where the comma indicates the partial derivative with respect to the subsequent quantity.

In the slow-roll regime, namely $\dot{\rho}_r \ll 4H\rho_r$, $\Gamma\dot{\phi}^2$ and $\ddot{\phi} \ll 3H\dot{\phi}$, $V_{,\phi}$, the background equations can be approximated as

$$3H^2 \simeq M_P^{-2}V, \quad (7)$$

$$4\rho_r \simeq 3Q\dot{\phi}^2, \quad (8)$$

$$3H(1 + Q)\dot{\phi} + V_{,\phi} \simeq 0, \quad (9)$$

where the parameter $Q \equiv \Gamma/(3H)$ measures the effectiveness of warm inflation. In particular, the strong regime of warm inflation is described by the condition $Q \gg 1$, while the weak regime occurs when $Q \ll 1$. One can then define the following slow-roll parameters [53]:

$$\epsilon_V = \frac{M_P^2}{2} \left(\frac{V_{,\phi}}{V} \right)^2, \quad (10)$$

$$\eta_V = M_P^2 \left(\frac{V_{,\phi\phi}}{V} \right), \quad (11)$$

$$\beta_V = M_P^2 \left(\frac{\Gamma_{,\phi} V_{,\phi}}{\Gamma V} \right). \quad (12)$$

The slow-roll approximation is valid as long as the conditions $\epsilon_V \ll 1 + Q$, $\eta_V \ll 1 + Q$ and $\beta_V \ll 1 + Q$ are satisfied. We remark that the parameter β_V is distinctive of the warm inflation scenario, and quantifies the possible dependence of Γ on the amplitude of the inflaton.

The occurrence of warm inflation relies on the condition $T > H$. Under such circumstances, thermal fluctuations of the inflaton field become dominant, implying that fluctuations in radiation's temperature are transmitted to the inflaton in the form of adiabatic curvature fluctuations. This differs significantly from the cold inflation

picture, in which the initial seeds for structure formation originate from quantum fluctuations. As a consequence, in the case of an explicit dependence of the dissipation coefficient on the temperature, it can be shown that the curvature power spectrum is given as [54]

$$\mathcal{P}_{\mathcal{R}} = \left(\frac{H_*^2}{2\pi\dot{\phi}_*} \right)^2 \left[1 + 2n_{\text{BE}} + \left(\frac{T_*}{H_*} \right) \frac{2\pi\sqrt{3}Q_*}{\sqrt{3+4\pi Q_*}} \right] \mathcal{F}(Q_*), \quad (13)$$

where the subindex ‘ \star ’ refers to the quantities evaluated at the horizon crossing, i.e., when $k = aH$. Here, $n_{\text{BE}} = (e^{H_*/T_*} - 1)^{-1}$ refers to the Bose-Einstein distribution of the inflaton under a thermal equilibrium of the radiation bath. Additionally, the function $\mathcal{F}(Q_*)$ measures the growth of perturbations of the inflaton coupled with radiation and can be determined numerically. Specifically, assuming $\Gamma \propto T$, one finds [18, 55]

$$\mathcal{F}(Q_*) \simeq 1 + 0.335Q_*^{1.364} + 0.0185Q_*^{2.315}. \quad (14)$$

It is worth noting that Eq. (13) reproduces the standard cold inflation expression for $(n, T, Q) \rightarrow 0$. Then, adopting the usual definition in the framework of cold inflation, one can obtain the scalar spectral index as [11]

$$\begin{aligned} n_s - 1 &\equiv \lim_{k \rightarrow k_0} \frac{d \ln \mathcal{P}_{\mathcal{R}}}{d \ln k} \\ &\simeq \frac{1}{1+Q} \left\{ -4\epsilon_V + 2 \left(\eta_V - \beta_V + \frac{\beta_V - \epsilon_V}{1+Q} \right) \right. \\ &\quad - \frac{\mathcal{A}}{1+\mathcal{A}} \left[\frac{6+(3+4\pi)Q}{(1+Q)(3+4\pi Q)} (\beta_V - \epsilon_V) \right. \\ &\quad \left. \left. + \frac{2\eta_V + \beta_V - 7\epsilon_V}{4} \right] \right\}, \end{aligned} \quad (15)$$

where k_0 is the pivot scale, and we have defined

$$\mathcal{A} \equiv \left(\frac{T}{H} \right) \frac{2\pi\sqrt{3}Q}{\sqrt{3+4\pi Q}}. \quad (16)$$

The standard cold inflation expression, $n_s = 1 - 6\epsilon_V + 2\eta_V$, is recovered in the limit $(T, Q) \rightarrow 0$.

On the other hand, the dissipation effects of warm inflation have a negligible impact on the primordial tensor perturbations of the metric. Therefore, the tensor power spectrum can be written as in the case of cold inflation:

$$\mathcal{P}_T = 2 \left(\frac{H_*}{\pi M_P} \right)^2. \quad (17)$$

Analogously to the scalar spectral index, we obtain the tensor spectral index as

$$n_T \equiv \lim_{k \rightarrow k_0} \frac{d \ln \mathcal{P}_T}{d \ln k} = -2\epsilon_V. \quad (18)$$

Finally, the tensor-to-scalar ratio is given by

$$r \equiv \frac{\mathcal{P}_T}{\mathcal{P}_{\mathcal{R}}} = \frac{16\epsilon_V}{(1+Q)\mathcal{F}(Q)} \left[1 + 2n + \left(\frac{T}{H} \right) \frac{2\pi\sqrt{3}Q}{\sqrt{3+4\pi Q}} \right]^{-1}. \quad (19)$$

Notice that all the spectral quantities are intended to be evaluated at the horizon crossing, as follows from Eq. (13).

III. SCALAR-INDUCED GW POWER SPECTRUM

To evaluate the spectrum of primordial GWs induced by scalar perturbations, we write down the perturbed FLRW metric in the Newtonian gauge [56]:

$$ds^2 = a(\eta)^2 \left\{ -(1+2\Phi)d\eta^2 + \left[(1-2\Phi)\delta_{ij} + \frac{1}{2}h_{ij} \right] dx^i dx^j \right\} \quad (20)$$

where $\eta \equiv \int \frac{dt}{a}$ is the conformal time, and h_{ij} are second-order tensor perturbations. Here, we neglected vector perturbations and the anisotropic stress, and Φ is the first-order Bardeen potential. In the Fourier space, one has

$$h_{ij}(\eta, \mathbf{x}) = \int \frac{d^3k}{(2\pi)^{3/2}} [h_{\mathbf{k}}^+(\eta)e_{ij}^+(\mathbf{k}) + h_{\mathbf{k}}^\times(\eta)e_{ij}^\times(\mathbf{k})] e^{i\mathbf{k}\cdot\mathbf{x}}, \quad (21)$$

where the transverse, traceless polarization tensors have been introduced:

$$e_{ij}^+(\mathbf{k}) \equiv \frac{1}{\sqrt{2}} [e_i(\mathbf{k})e_j(\mathbf{k}) - \bar{e}_i(\mathbf{k})\bar{e}_j(\mathbf{k})], \quad (22)$$

$$e_{ij}^\times(\mathbf{k}) \equiv \frac{1}{\sqrt{2}} [e_i(\mathbf{k})\bar{e}_j(\mathbf{k}) - \bar{e}_i(\mathbf{k})e_j(\mathbf{k})], \quad (23)$$

with $e_i(\mathbf{k})$ and $\bar{e}_i(\mathbf{k})$ being orthonormal basis vectors that are orthogonal to the comoving momentum \mathbf{k} . Moreover, $k \equiv |\mathbf{k}|$ and $\lambda = \{+, \times\}$ is the polarization index which will be dropped in the following¹. The evolution equation for the amplitude of the scalar-induced GWs is given by

$$h_{\mathbf{k}}''(\eta) + 2\mathcal{H}h_{\mathbf{k}}'(\eta) + k^2h_{\mathbf{k}}(\eta) = \mathcal{S}_{\mathbf{k}}(\eta), \quad (24)$$

where $\mathcal{H} \equiv aH$ is the conformal Hubble parameter, and the prime denotes the derivative with respect to η .

In the case of adiabatic perturbations² in a universe dominated by relativistic matter with an equation of state $p = w\rho$, the evolution equation for the gravitational potential reads [57]

$$\Phi_{\mathbf{k}}'' + \frac{6}{\eta} \left(\frac{1+w}{1+3w} \right) \Phi_{\mathbf{k}}' + wk^2\Phi_{\mathbf{k}} = 0, \quad (25)$$

whose solution is

$$\Phi_{\mathbf{k}} = \eta^{-\nu} [c_1 J_\nu(k\eta\sqrt{w}) + c_2 Y_\nu(k\eta\sqrt{w})], \quad (26)$$

¹ Under parity invariance, both polarizations give the same result.

² In the absence of entropy, the pressure fluctuations are given by $\delta p = c_s^2 \delta \rho$, where $c_s^2 = w$ is the squared adiabatic speed of sound.

with $\nu \equiv \frac{5+3w}{2(1+3w)}$. Here, c_1 and c_2 are arbitrary constants, while J_ν and Y_ν are ν -order Bessel functions. Hence, the source term $\mathcal{S}_{\mathbf{k}}(\eta)$ can be written as [58, 59]

$$\mathcal{S}_{\mathbf{k}} = \frac{4e^{ij}(\mathbf{k})}{(2\pi)^{3/2}} \int d^3q q_i q_j \left[2\Phi_{\mathbf{k}-\mathbf{q}} \Phi_{\mathbf{q}} + \frac{4}{3(1+w)} (\mathcal{H}^{-1}\Phi'_{\mathbf{k}-\mathbf{q}} + \Phi_{\mathbf{k}-\mathbf{q}}) (\mathcal{H}^{-1}\Phi'_{\mathbf{q}} + \Phi_{\mathbf{q}}) \right]. \quad (27)$$

The solution for $h_{\mathbf{k}}(\eta)$ can be found by using the Green's function method. Specifically, one has

$$h_{\mathbf{k}}(\eta) = \frac{1}{a(\eta)} \int_{\eta}^{\eta} d\tilde{\eta} G_{\mathbf{k}}(\eta, \tilde{\eta}) a(\tilde{\eta}) \mathcal{S}_{\mathbf{k}}(\tilde{\eta}), \quad (28)$$

where $G_{\mathbf{k}}(\eta, \tilde{\eta})$ satisfies the following equation:

$$G''_{\mathbf{k}}(\eta, \tilde{\eta}) + \left[k^2 - \frac{a''(\eta)}{a(\eta)} \right] G_{\mathbf{k}}(\eta, \tilde{\eta}) = \delta(\eta - \tilde{\eta}). \quad (29)$$

Then, the power spectrum \mathcal{P}_h of the induced GWs is defined as

$$\langle h_{\mathbf{k}}(\eta) h_{\mathbf{k}_1}(\eta) \rangle = \frac{2\pi^2}{k^3} \delta(\mathbf{k} + \mathbf{k}_1) \mathcal{P}_h(k, \eta). \quad (30)$$

Following the calculations detailed in [58–60], one finds

$$\mathcal{P}_h(k, \eta) = 4 \int_0^\infty dv \int_{|1-v|}^{1+v} du \left[\frac{4v^2 - (1+v^2 - u^2)^2}{4uv} \right]^2 \times I^2(v, u, y) \mathcal{P}_{\mathcal{R}}(kv) \mathcal{P}_{\mathcal{R}}(ku), \quad (31)$$

where $u \equiv |\mathbf{k} - \mathbf{k}_1|/k$, $v \equiv k_1/k$ and $y \equiv k\eta$. Here,

$$I(v, u, y) = \int_0^y d\tilde{y} \frac{a(\tilde{y})}{a(y)} k G_{\mathbf{k}}(y, \tilde{y}) f(v, u, \tilde{y}), \quad (32)$$

and

$$\begin{aligned} f(v, u, \tilde{y}) &= \frac{3(1+w)(1+3w)^2}{(3w+5)^2} \tilde{y}^2 \Phi'(v\tilde{y}) \Phi'(u\tilde{y}) \\ &+ \frac{6(1+3w)(1+w)}{(3w+5)^2} [\tilde{y} \Phi'(v\tilde{y}) \Phi(u\tilde{y}) + \tilde{y} \Phi(v\tilde{y}) \Phi'(u\tilde{y})] \\ &+ \frac{6(1+w)}{3w+5} \Phi(v\tilde{y}) \Phi(u\tilde{y}), \end{aligned} \quad (33)$$

where we considered $\Phi_{\mathbf{k}} = \Phi(k\eta)\varphi_{\mathbf{k}}$, with $\Phi(k\eta)$ being the transfer function, and $\varphi_{\mathbf{k}}$ are the primordial values of the fluctuations before entering the horizon. The latter obey the relation

$$\langle \varphi_{\mathbf{k}} \varphi_{\mathbf{k}_1} \rangle = \frac{2\pi^2}{k^3} \left(\frac{3+3w}{5+3w} \right)^2 \delta(\mathbf{k} + \mathbf{k}_1) \mathcal{P}_{\mathcal{R}}(k). \quad (34)$$

The power spectrum can be related to the GW energy density. In particular, for subhorizon modes we have

$$\rho_{\text{GW}} = \left(\frac{M_P}{4a} \right)^2 \overline{\langle h_{ij,k} h_{ij,k} \rangle}, \quad (35)$$

where the bar indicates the average over oscillations. Therefore, we can calculate the GW energy density as

$$\Omega_{\text{GW}}(k, \eta) \equiv \frac{\rho_{\text{GW}}(\eta, k)}{\rho_{\text{cr}}(\eta)} = \frac{1}{24} \left(\frac{k}{a(\eta)H(\eta)} \right)^2 \overline{P_h(k, \eta)}, \quad (36)$$

where $\rho_{\text{cr}} = 3M_P^2 H^2$ is the universe's critical density.

A. Radiation-dominated era

We shall consider GWs produced during the radiation-dominated era. In this case, one has $w = 1/3$, $a \propto \eta$ and $\mathcal{H} = \eta^{-1}$. Therefore, the general solution of Eq. (25) is

$$\Phi(y) = \frac{1}{y^2} \left\{ c_1 \left[\frac{\sin(y/\sqrt{3})}{y/\sqrt{3}} - \cos(y/\sqrt{3}) \right] + c_2 \left[\frac{\cos(y/\sqrt{3})}{y/\sqrt{3}} + \sin(y/\sqrt{3}) \right] \right\}, \quad (37)$$

Requiring the gravitational potential to approach unity at early times ($y \rightarrow 0$), we select the solution

$$\Phi(y) = \frac{9}{y^2} \left[\frac{\sin(y/\sqrt{3})}{y/\sqrt{3}} - \cos(y/\sqrt{3}) \right]. \quad (38)$$

On the other hand, solving Eq. (29) yields

$$G_{\mathbf{k}}(y, \tilde{y}) = \frac{1}{k} \sin(y - \tilde{y}). \quad (39)$$

From Eq. (36), we then obtain [59]

$$\begin{aligned} \Omega_{\text{GW}}(k) &= \frac{1}{12} \int_0^\infty dv \int_{|1-v|}^{1+v} du \left[\frac{4v^2 - (1 - u^2 + v^2)^2}{4uv} \right]^2 \left[\frac{3(u^2 + v^2 - 3)}{4u^3 v^3} \right]^2 \left\{ \left[(u^2 + v^2 - 3) \ln \left| \frac{3 - (u+v)^2}{3 - (u-v)^2} \right| - 4uv \right]^2 \right. \\ &\quad \left. + \pi^2 (u^2 + v^2 - 3)^2 \Theta(u + v - \sqrt{3}) \right\} \mathcal{P}_{\mathcal{R}}(kv) \mathcal{P}_{\mathcal{R}}(ku), \end{aligned} \quad (40)$$

where Θ is the Heaviside theta function.

Finally, the present amount of scalar-induced GWs is

given by [46]

$$\Omega_{\text{GW},0}(k) = \Omega_{r,0} \left(\frac{g_{\text{eff}}(k)}{g_{\text{eff},0}} \right) \left(\frac{g_{\text{eff},s0}}{g_{\text{eff},s}(k)} \right)^{4/3} \Omega_{\text{GW}}(k), \quad (41)$$

where $\frac{\Omega_{r,0}}{g_{\text{eff},0}} \simeq 2.72 \times 10^{-5}$ is the current radiation density per relativistic degrees of freedom. Here, g_{eff} and $g_{\text{eff},s}$ are the effective number of relativistic degrees of freedom contributing to the energy and entropy densities, respectively, whose values are taken from Ref. [61]. Additionally, $g_{\text{eff},s0} \simeq 3.93$ indicates the present amount of the effective number of relativistic degrees of freedom contributing to entropy.

IV. ANALYSIS OF INFLATIONARY POTENTIALS

In the following, we specialize our study on chaotic and exponential potentials to obtain the analytic form of the curvature power spectrum. To evaluate the integral in Eq. (40), we follow the strategy adopted in Ref. [59] and we look for a power-law spectrum of the form

$$\mathcal{P}_{\mathcal{R}} = A_s \left(\frac{k}{k_*} \right)^{n_s - 1}. \quad (42)$$

Here, the amplitude A_s and the scalar spectral index n_s are dependent on specific potential models, while k_* is the pivot scale. A similar approach has been recently used in Ref. [46], where the power spectrum is modeled by a Dirac delta function, Gaussian peak and a box function in logarithmic k space. In this way, Eq. (40) can be readily computed, and one can compare the predictions of warm inflation directly with the CMB-Planck results [62].

A. Chaotic potentials

Let us start by considering the chaotic inflationary potential [63, 64]

$$V(\phi) = \frac{\lambda M_P^4}{\alpha} \left(\frac{\phi}{M_P} \right)^\alpha, \quad (43)$$

where $\alpha = 2k$, with $k \in \mathbb{Z}^+$, and λ is a dimensionless constant measuring the degree of flatness in the potential. Combining Eqs. (7) and (9) in the slow-roll regime we then get

$$\left(\frac{H^2}{2\pi\dot{\phi}} \right)^2 \simeq \frac{\lambda(1+Q)^2}{12\pi^2\alpha^3} \left(\frac{\phi}{M_P} \right)^{2+\alpha}. \quad (44)$$

Additionally, from Eq. (8) and recalling the temperature dependence of the radiation energy density, we find

$$\frac{T}{H} \simeq \left[\frac{135 Q \alpha^3}{2\pi^2 g_{\text{eff}} \lambda (1+Q)^2} \right]^{1/4} \left(\frac{M_P}{\phi} \right)^{\frac{2+\alpha}{4}}. \quad (45)$$

Given the potential (43), one can also calculate the expressions of the slow-roll parameters. In particular, Eq. (10) reads

$$\epsilon_V = \frac{1}{2} \left(\frac{\alpha M_P}{\phi} \right)^2. \quad (46)$$

The condition $\epsilon_V \simeq 1 + Q$ provides us with an estimate of ϕ at the end of inflation:

$$\phi_{\text{end}} \simeq \frac{\alpha M_P}{\sqrt{2(1+Q)}}. \quad (47)$$

On the other hand, the value of ϕ at the horizon crossing can be obtained from the number of e-folds:

$$N_e = \int_{t_*}^{t_{\text{end}}} H dt \simeq -\frac{1}{M_P^2} \int_{\phi_*}^{\phi_{\text{end}}} \frac{V}{V'} (1+Q) d\phi, \quad (48)$$

where Eqs. (7) and (9) have been used in the last equality. Therefore, for the potential (43), we find

$$\phi_* \simeq M_P \sqrt{\frac{\alpha(\alpha + 4N_e)}{2(1+Q_*)}}. \quad (49)$$

The latter can be used to express Eqs. (44) and (45) at the time of horizon crossing. Specifically, we obtain

$$\left(\frac{H_*^2}{2\pi\dot{\phi}_*} \right)^2 \simeq \frac{5(1+Q_*)^{1-\alpha/2}}{8\pi^4 g_{\text{eff}} x_\alpha^4}, \quad (50)$$

and

$$\frac{T_*}{H_*} \simeq \sqrt{3} \left[Q_* (1+Q_*)^{\alpha/2-1} \right]^{1/4} x_\alpha, \quad (51)$$

where we have introduced the auxiliary variable

$$x_\alpha \equiv \left[\frac{15 \alpha^{2-\alpha/2} 2^{\alpha/2}}{\pi^2 g_{\text{eff}} \lambda (\alpha + 4N_e)^{1+\alpha/2}} \right]^{1/4}. \quad (52)$$

To express the dissipation parameter in terms of the inflationary model, we assume a weak regime of warm inflation ($Q \ll 1$), and set $\Gamma = c_1 T$, with c_1 being a dimensionless constant [20]. In so doing, we can expand Eq. (51) up to the first order and use the relation $Q = \frac{c_1 T}{3H}$ to obtain

$$Q_* \approx \left(\frac{c_1^4 x_\alpha^4}{9} \right)^{1/3}. \quad (53)$$

Inverting the above relation to express x_α in terms of the dissipation parameter, from Eqs. (50) and (51) we obtain, respectively,

$$\left(\frac{H_*^2}{2\pi\dot{\phi}_*} \right)^2 \approx \frac{5c_1^4 (1+Q_*)^{1-\alpha/2}}{72 \pi^4 g_{\text{eff}} Q_*^3}, \quad (54)$$

and

$$\frac{T_*}{H_*} \approx \frac{3Q_*}{c_1}. \quad (55)$$

Therefore, the amplitude of the curvature power spectrum reads

$$A_s \approx \frac{5c_1^4 \mathcal{F}(Q_*) (1+Q_*)^{1-\frac{\alpha}{2}}}{72\pi^4 g_{\text{eff}} Q_*^3} \left[\coth\left(\frac{c_1}{6Q_*}\right) + \frac{6\pi\sqrt{3}Q_*^2}{c_1\sqrt{3+4\pi Q_*}} \right]. \quad (56)$$

Moreover, in the weak dissipation limit, Eq. (15) can be approximated as

$$n_s \approx 1 - 6\epsilon_V + 2\eta_V + 2Q_* \left[4\epsilon_V - \beta_V - \eta_V - \frac{\pi}{4} \frac{T_*}{H_*} (9\beta_V + 2\eta_V - 15\epsilon_V) \right]. \quad (57)$$

Using Eqs. (10)–(12) for the potential (43), with the help of Eqs. (53) and (55), we obtain

$$n_s \approx 1 + \frac{1+Q_*}{2c_1(\alpha+4N_e)} \left[8c_1(1+\alpha)Q_* - 4c_1(2+\alpha) + 3\pi(4+11\alpha)Q_*^2 \right]. \quad (58)$$

Notice that, in the limit $Q_* \rightarrow 0$, the above result yields

$$n_s \approx 1 - \frac{2+\alpha}{2N_e}, \quad (59)$$

consistently with the predictions of cold inflation [52].

1. Quadratic potential

In the case of $\alpha = 2$, Eq. (52) reads

$$x_2 = \sqrt{\frac{2}{\pi(2+4N_e)}} \left(\frac{15}{g_{\text{eff}}\lambda} \right)^{1/4}, \quad (60)$$

so that, from Eq. (53), one finds

$$Q_* \approx \left[\frac{5c_1^4}{3\pi^2 g_{\text{eff}}\lambda(1+2N_e)^2} \right]^{1/3}. \quad (61)$$

The latter can be used to compute the amplitude and the spectral index of the power spectrum. Specifically, Eq. (56) and (58) become, respectively:

$$A_s \approx \frac{5c_1^3 \mathcal{F}(Q_*)}{72\pi^4 g_{\text{eff}} Q_*^3} \left[c_1 \coth\left(\frac{c_1}{6Q_*}\right) + \frac{6\pi\sqrt{3}Q_*^2}{\sqrt{3+4\pi Q_*}} \right], \quad (62)$$

$$n_s \approx 1 + \frac{(1+Q_*) [39\pi Q_*^2 + 4c_1(3Q_* - 2)]}{2c_1(1+2N_e)}. \quad (63)$$

2. Quartic potential

For $\alpha = 4$, Eq. (52) becomes

$$x_4 = \frac{1}{2\sqrt{\pi}} \left[\frac{15}{g_{\text{eff}}\lambda(1+N_e)^3} \right]^{1/4}, \quad (64)$$

and, from Eq. (53), we have

$$Q_* \approx \frac{1}{1+N_e} \left(\frac{5c_1^4}{48\pi^2 g_{\text{eff}}\lambda} \right)^{1/3}. \quad (65)$$

In this case, the amplitude of the power spectrum reads

$$A_s \approx \frac{5c_1^3 \mathcal{F}(Q_*)}{72\pi^4 g_{\text{eff}} Q_*^3 (1+Q_*)} \left[c_1 \coth\left(\frac{c_1}{6Q_*}\right) + \frac{6\pi\sqrt{3}Q_*^2}{\sqrt{3+4\pi Q_*}} \right], \quad (66)$$

while the scalar index is given by

$$n_s \approx \frac{18\pi Q_*^2 (1+Q_*) + c_1 [N_e - 2 + Q_*(2+5Q_*)]}{c_1(1+N_e)}. \quad (67)$$

B. Exponential potential

As a second class of inflationary potentials, we consider the exponential model [65–67]

$$V(\phi) = \frac{\lambda M_P^4}{\alpha} e^{-\beta\left(\frac{\phi}{M_P}\right)^\alpha}, \quad (68)$$

where $\{\alpha, \beta\} \in \mathbb{R}$, with $\beta > 0$. It is worth noting that the $\alpha > 1$ cases are characterized by the absence of the graceful exit problem even in the conventional cold inflation picture. Moreover, for $\alpha = 1$, one would obtain an excessively red-tilted spectrum in the warm inflation scenario [68]. Therefore, we shall study the cases where $\alpha > 1$ in the following.

Under the slow-roll approximation, we get

$$\left(\frac{H}{2\pi\dot{\phi}} \right)^2 \simeq \frac{\lambda}{3\alpha} \left(\frac{1+Q}{2\pi\alpha\beta} \right)^2 \left(\frac{\phi}{M_P} \right)^{2(1-\alpha)} e^{-\beta\left(\frac{\phi}{M_P}\right)^\alpha}, \quad (69)$$

and

$$\frac{T}{H} \simeq \left[\frac{135 Q \alpha^3 \beta^2}{2\pi^2 g_{\text{eff}}\lambda(1+Q)^2} \right]^{1/4} \left(\frac{M_P}{\phi} \right)^{\frac{1-\alpha}{2}} e^{\frac{\beta}{4}\left(\frac{\phi}{M_P}\right)^\alpha}. \quad (70)$$

At the end of inflation, one has

$$\epsilon_V = \frac{\alpha^2 \beta^2}{2} \left(\frac{\phi}{M_P} \right)^{2(\alpha-1)} \simeq 1 + Q, \quad (71)$$

leading to

$$\phi_{\text{end}} \simeq M_P \left[\frac{2(1+Q)}{\alpha^2 \beta^2} \right]^{\frac{1}{2(\alpha-1)}}. \quad (72)$$

Additionally, inverting Eq. (48) for the potential (68), we find the value of the inflaton at the horizon crossing:

$$\phi_* \simeq M_P \xi_1^{1/\alpha}, \quad (73)$$

where $\alpha \neq 2$, and

$$\xi_1 \equiv \left\{ \alpha\beta(\alpha-2)N_e + (\alpha\beta)^{\frac{2-\alpha}{1-\alpha}} [2(1+Q_*)]^{\frac{\alpha-2}{2(1-\alpha)}} \right\}^{\frac{\alpha}{2-\alpha}}. \quad (74)$$

Hence, one gets:

$$\left(\frac{H_\star^2}{2\pi\dot{\phi}_\star}\right)^2 \simeq \frac{\lambda}{3\alpha} \left(\frac{1+Q_\star}{2\pi\alpha\beta\xi_1^{1-1/\alpha}}\right)^2 e^{-\beta\xi_1}, \quad (75)$$

$$\frac{T_\star}{H_\star} \simeq \left[\frac{135\alpha^3\beta^2Q_\star\xi_1^{2-2/\alpha}e^{\beta\xi_1}}{2\pi^2g_{\text{eff}}\lambda(1+Q_\star)^2}\right]^{1/4}. \quad (76)$$

In the weak dissipation regime, for $\Gamma = c_1T$, we obtain

$$Q_\star \approx \left(\frac{5c_1^4\alpha^3\beta^2}{6\pi^2g_{\text{eff}}\lambda}\right)^{1/3} \xi_2^{-\frac{2}{3}(\frac{\alpha-1}{\alpha-2})} e^{\frac{\beta}{3}\xi_2^{\frac{2-\alpha}{\alpha}}}, \quad (77)$$

where³

$$\xi_2 \equiv \left(\frac{\alpha\beta}{\sqrt{2}}\right)^{\frac{2-\alpha}{1-\alpha}} + \alpha\beta(\alpha-2)N_e. \quad (78)$$

The amplitude of the power spectrum is then

$$A_s \approx \frac{\lambda(1+Q_\star)^2\mathcal{F}(Q_\star)}{12\pi^2\alpha^3\beta^2\xi_1^{2-\frac{2}{\alpha}}e^{\beta\xi_1}} \left\{ \coth \left[\frac{1}{2} \left(\frac{2\pi^2g_{\text{eff}}\lambda(1+Q_\star)^2}{135\alpha^3\beta^2Q_\star\xi_1^{2-\frac{2}{\alpha}}e^{\beta\xi_1}} \right)^{\frac{1}{4}} \right] + \frac{3}{\sqrt{3+4\pi Q_\star}} \left[\frac{120\pi^2\alpha^3\beta^2Q_\star^5\xi_1^{2-\frac{2}{\alpha}}e^{\beta\xi_1}}{g_{\text{eff}}\lambda(1+Q_\star)^2} \right]^{\frac{1}{4}} \right\}, \quad (79)$$

while the spectral index is given by

$$n_s \approx 1 + \frac{\alpha\beta}{8}\xi_1^{\frac{\alpha-2}{\alpha}} \left\{ 16 - 8\alpha(2 + \beta\xi_1) + 16Q_\star[\alpha(1 + \beta\xi_1) - 1] + Q_\star[\alpha(4 + 11\beta\xi_1) - 4] \left[\frac{1080\pi^2\alpha^3\beta^2Q_\star^5\xi_1^{2-\frac{2}{\alpha}}e^{\beta\xi_1}}{g_{\text{eff}}\lambda(Q+1)^2} \right]^{\frac{1}{4}} \right\}. \quad (80)$$

It can be shown that Eq. (80) recovers the cold inflation expression in the limit $Q_\star \rightarrow 0$.

V. NANOGRAV CONSTRAINTS

To test the aforementioned warm inflation models, we use the NANOGrav 15-yr dataset including the timing of pulses from 68 millisecond pulsars, measured as time of arrivals [46, 69]. For our purposes, we utilize the `ceffy` suite [70] and the package `PTArcade` [71] to conduct a Bayesian analysis on the NANOGrav dataset. The posterior distributions are thus obtained via the Markov Chain Monte Carlo (MCMC) numerical integration using the `PTMCMCSampler` software [72]. Specifically, we evaluate the integral in Eq. (40) through the parametrization

$$\Omega_{\text{GW}}(f) = Q(n_s)A_s^2 \left(\frac{f}{f_\star}\right)^{2(n_s-1)}, \quad (81)$$

where $f \equiv \frac{k}{2\pi}$ is the present GW frequency, and f_\star is the frequency corresponding to the pivot scale. Here, the function $Q(n_s)$ is computed numerically using the values provided in Table 1 of Ref. [59].

In the following, we present our numerical results for $N_e = 60$, in agreement with the Planck predictions [62].

Quadratic potential. In the case of the quadratic potential, we assume uniform priors in the logarithmic scale $[-16, -2]$, $[-8, -2]$ and $[-16, -2]$ for the parameters λ , c_1 and f_\star , respectively. In Fig. 1, we show the 1σ and 2σ contour plots obtained from the analysis of the GW background alone, and from the combination of the GW background and the astrophysical signal from inspiraling supermassive black hole binaries (SMBHBs). In the first row of Table I, we report the 2σ limits on the values of the c_1 , λ and f_\star parameters. In particular, the best-fit values are $\log_{10}\lambda = -12.0_{-2.8}^{+2.5}$ ($-11.1_{-5.3}^{+6.3}$), $\log_{10}c_1 = -2.44_{-1.10}^{+0.92}$ ($-3.9_{-3.6}^{+2.4}$) and $\log_{10}(f_\star/\text{Hz}) = -13.4_{-1.5}^{+1.5}$ ($-10.6_{-4.5}^{+7.1}$) for the GW background (GW background + SMBHB) signal.

Quartic potential. For the quartic potential, we assume the uniform priors $\log_{10}\lambda \in [-16, -2]$, $\log_{10}c_1 \in [-7, -2]$ and $\log_{10}(f_\star/\text{Hz}) \in [-15, -2]$. Then, in Fig. 1, we show the 1σ and 2σ contour plots and the posterior distributions from the analysis of the GW background and the GW background + SMBHB signal. The 95% confidence level (C.L.) limits on λ , c_1 and f_\star parameters are presented in the second row of Table I. In particular, we obtain $\lambda < 1.23 \times 10^{-14}$ (3.9×10^{-8}), $\log_{10}c_1 = -2.51_{-0.49}^{+0.47}$ ($-3.2_{-2.5}^{+1.3}$) and $\log_{10}(f_\star/\text{Hz}) = -8.0_{-2.8}^{+2.9}$ ($-7.9_{-2.9}^{+2.8}$) for the GW background (GW background + SMBHB) signal. Our constraints are compatible with the theoretical limits $\lambda \lesssim 10^{-8}$ required to achieve a successful inflation scenario [73].

³ Notice that $\xi_1 \rightarrow \xi_2$ in the limit $Q_\star \rightarrow 0$.

Potential	α	$\log_{10} \beta$	$\log_{10} c_1$	$\log_{10} \lambda$	$\log_{10}(f_*/\text{Hz})$
Quadratic	2	-	$-2.44^{+0.92}_{-1.10}$ ($-3.9^{+2.4}_{-3.6}$)	$-12.0^{+2.5}_{-2.8}$ ($-11.1^{+6.3}_{-5.3}$)	$-13.4^{+1.5}_{-1.5}$ ($-10.6^{+7.1}_{-4.5}$)
Quartic	4	-	$-2.51^{+0.47}_{-0.49}$ ($-3.2^{+1.3}_{-2.5}$)	< -13.91 (-7.40)	$-8.0^{+2.9}_{-2.8}$ ($-7.9^{+2.8}_{-2.9}$)
Exponential	$3.9^{+1.2}_{-1.3}$ ($4.2^{+1.7}_{-1.8}$)	$-1.7^{+1.3}_{-1.2}$ ($-2.0^{+1.9}_{-1.9}$)	$-2.8^{+1.1}_{-1.0}$ ($-2.7^{+1.2}_{-1.2}$)	$-12.9^{+3.3}_{-3.0}$ ($-12.3^{+4.1}_{-3.8}$)	$-9.2^{+3.4}_{-1.9}$ ($-8.2^{+3.0}_{-2.7}$)

TABLE I. Summary of our constraints on the warm inflationary models. The best-fit values and 2σ uncertainties are provided for the quadratic, quartic and exponential potential parameters. The values in parentheses indicate the results obtained when the SMBHB signal is added to the GW background.

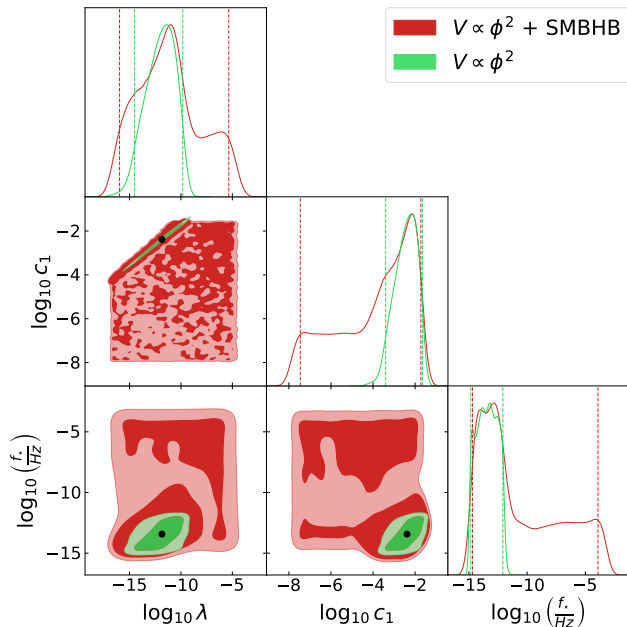


FIG. 1. Marginalized 68% and 95% C.L. contours, with posterior distributions, for the free parameters of the quadratic potential model. The dashed lines indicate the 95% C.L. limits, while the black dot corresponds to the maximum likelihood values for the GW background signal only.

Exponential potential. In the case of the exponential potential, we assume the priors to be uniform in the following intervals: $\log_{10} \lambda \in [-16, -2]$, $\log_{10} c_1 \in [-4, 0]$, $\alpha \in [1, 5]$, $\beta \in [10^{-4}, 1]$ and $\log_{10}(f_*/\text{Hz}) \in [-12, -5]$. The best-fit values and 1σ uncertainties we obtain are listed in the last row of Table I. Additionally, in Fig. 3, we display the 1σ and 2σ contour plots, and the posterior distributions, for the GW background alone and the GW background + SMBHB signal.

A. Model selection

To evaluate the statistical performance of the different models, we make use of the Bayesian inference method [74]. Given a dataset \mathcal{D} , the posterior probability distribution for a model \mathcal{M} characterized by a set of parameters θ can be written as

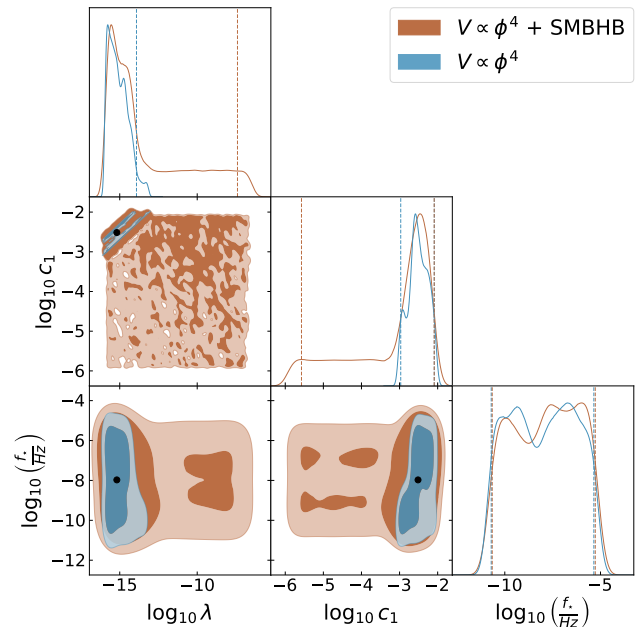


FIG. 2. Marginalized 68% and 95% C.L. contours, with posterior distributions, for the free parameters of the quartic potential model. The dashed lines indicate the upper 95% C.L. limits, while the black dot corresponds to the maximum likelihood values for the GW background signal only.

$$P(\theta|\mathcal{D}, \mathcal{M}) = \frac{P(\mathcal{D}|\theta, \mathcal{M})P(\theta|\mathcal{M})}{P(\mathcal{D}|\mathcal{M})}, \quad (82)$$

where $P(\mathcal{D}|\theta, \mathcal{M})$ and $P(\theta|\mathcal{M})$ are the likelihood and the prior probability distributions, respectively. Here,

$$P(\mathcal{D}|\mathcal{M}) = \int d\theta P(\mathcal{D}|\theta, \mathcal{M})P(\theta|\mathcal{M}) \quad (83)$$

is the marginalized likelihood, i.e. the Bayesian evidence. Thus, two models \mathcal{M}_1 and \mathcal{M}_2 can be compared through the Bayes factor, defined as

$$\mathcal{B}_{1,2} = \frac{P(\mathcal{D}|\mathcal{M}_1)}{P(\mathcal{D}|\mathcal{M}_2)}. \quad (84)$$

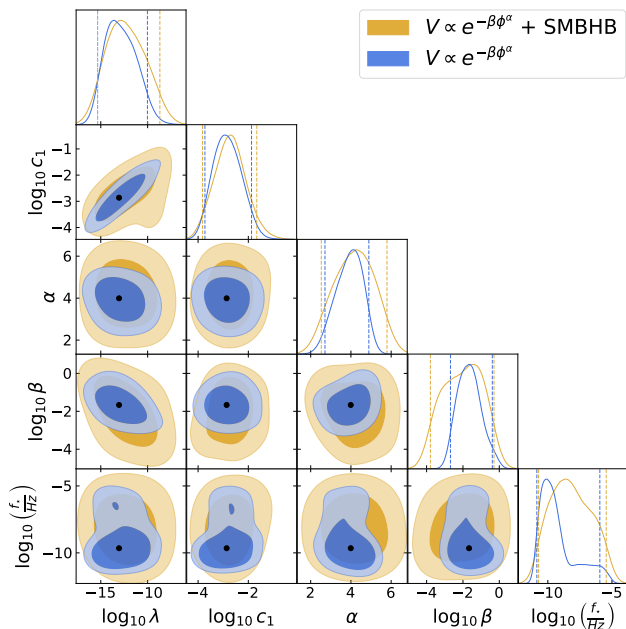


FIG. 3. Marginalized 68% and 95% C.L. contours, with posterior distributions, for the free parameters of the exponential potential model. The dashed lines indicate the 95% C.L. limits, while the black dot corresponds to the best-fit values for the GW background signal only.

The Bayes factor's value indicates whether the model \mathcal{M}_1 is favored or opposed compared to the model reference \mathcal{M}_2 , according to the Jeffrey scale [75]: for $\log_{10} \mathcal{B}_{1,2} < 0$, \mathcal{M}_1 is disfavored, while $\log_{10} \mathcal{B}_{1,2} \in [0, 0.5]$, $[0.5, 1]$, $[1, 1.5]$ $[1.5, 2]$ and $[2, \infty)$ mean weak, substantial, strong, very strong and decisive evidence for \mathcal{M}_1 , respectively.

In our case, we choose the quadratic potential as the reference model. Then, we obtain $\log_{10} \mathcal{B} = -0.01, 0.1$ for the quartic and exponential potentials, respectively. This means that the exponential model is slightly favored, while the quartic potential model performs statistically as well as the quadratic potential scenario.

Finally, in Fig. 4, we compare the GW spectrum inferred from the different inflationary potentials under investigation with the NANOGrav data. In particular, the curves are obtained using the maximum likelihood values for the parameters of the chaotic potentials and the best-fit values for the parameters of the exponential potential.

B. Comparison with CMB observations

We here discuss our findings in light of the predictions from the CMB measurements by the Planck collaboration. For this purpose, we use the maximum likelihood values for the free parameters of the inflationary models under study (see Table I) to estimate the dissipation coefficient, which in turn allows us to obtain the scalar spectral index. In particular, we find $Q_* = \{0.08, 0.04, 0.04\}$ for the quadratic, quartic and exponential models, re-

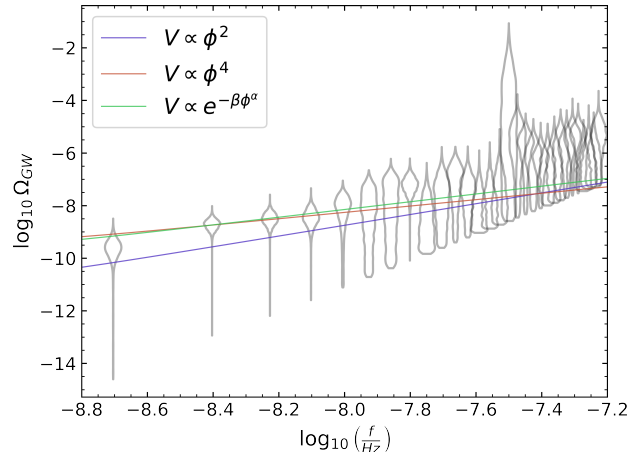


FIG. 4. The gray regions indicate the posteriors of a Hellings-Downs correlated free spectral reconstruction of the NANOGrav signal, while the solid lines refer to the GW background spectrum inferred from the warm inflationary models. The curves are obtained from the best-fit values of the free parameters of the inflationary potential models under study.

spectively. This is consistent with the working hypothesis of a weak dissipation regime of inflation.

As a consequence, we obtain $n_s = \{2.01, 1.61, 1.74\}$ for the quadratic, quartic and exponential models, respectively. Our results indicate a blue-tilted spectrum that is in tension with the Planck-CMB estimate [76]. This effect is generally expected as GWs produced by cosmic inflation could be observed at nHz frequencies in the case of a blue-tilted spectrum [77]. A similar behavior is known to occur for scalar-induced GWs produced during inflation [45].

Furthermore, we repeat our MCMC analysis to take into account the lower bound on the e-fold number considered by Planck [76], namely $N_e = 50$. The corresponding results are summarized in Table II. We notice no substantial differences compared the case with $N_e = 60$, as all the constraints on the model parameters are consistent within 1σ C.L. with the results reported in Table I.

VI. SUMMARY AND PERSPECTIVES

In this work, we examined the warm inflationary scenario within a spatially flat FLRW background. We investigated the primordial universe where the cosmic fluid is made of radiation and a canonical scalar field responsible for the inflationary dynamics. Specifically, we assumed an energy exchange between thermal fluctuations and the inflaton field, resulting in dissipation effects that facilitate a smooth transition to the radiation-dominated era. We thus took into account corrections to the curvature power spectrum with respect to the cold inflation picture, under the assumption of a linear dependence of

Potential	α	$\log_{10} \beta$	$\log_{10} c_1$	$\log_{10} \lambda$	$\log_{10}(f_*/\text{Hz})$
Quadratic	2	-	$-2.51^{+0.98}_{-1.1}$ ($-4.0^{+2.5}_{-3.7}$)	$-11.9^{+2.6}_{-2.9}$ ($-10.8^{+6.1}_{-5.6}$)	$-13.5^{+1.5}_{-1.5}$ ($-10.2^{+6.5}_{-4.6}$)
Quartic	4	-	$-2.62^{+0.47}_{-0.49}$ ($-3.3^{+1.3}_{-2.5}$)	< -13.11 (-7.00)	$-8.2^{+2.7}_{-2.9}$ ($-8.0^{+2.9}_{-2.8}$)
Exponential	$4.4^{+1.6}_{-1.6}$ ($4.4^{+1.8}_{-1.8}$)	$-1.5^{+1.6}_{-1.8}$ ($-1.9^{+1.9}_{-2.0}$)	$-2.7^{+1.1}_{-1.0}$ ($-2.7^{+1.5}_{-1.2}$)	$-12.9^{+3.0}_{-2.7}$ ($-11.4^{+7.5}_{-4.6}$)	$-7.6^{+2.9}_{-3.4}$ ($-7.9^{+2.8}_{-2.9}$)

TABLE II. Summary of the results from the analysis similar to that in Table I for $N_e = 50$.

the dissipation coefficient on the temperature of the radiation bath.

In particular, we focused on second-order tensor perturbations, sourced by scalar fluctuations that reentered the horizon after inflation. Thus, we computed the energy density of scalar-induced GWs in terms of a power-law parametrization of the primordial curvature power spectrum. We obtained analytical expressions for the latter under the slow-roll approximation by assuming a weak dissipation regime of warm inflation. To this end, we considered two classes of inflationary models, based on chaotic and exponential potentials of the inflaton.

Then, we tested the theoretical predictions for the present amount of GW energy density with the recent observations of a stochastic GW background signal from PTA measurements. For this aim, we performed an MCMC numerical analysis of the latest dataset released by the NANOGrav collaboration. We obtained 95% C.L. bounds on the free parameters of the inflationary models under investigation and the pivot scale of the PTAs, by considering both the GW background signal alone and the combination of the GW background with the astrophysical signal from an SMBHB population. We found that our constraints are in agreement with the theoretical limits necessary to achieve successful inflation. Based on the results of the MCMC analysis, we conducted a model selection study to assess the statistical performance of the different inflationary scenarios. Specifically, we found that the exponential potential model is slightly preferred, while the quadratic and quartic models are statistically indistinguishable.

Furthermore, we discussed and compared the outcomes of the present study with the most recent CMB observations by the Planck collaboration. In particular, we showed that our results indicate a blue-tilted power spectrum, consistently with previous nHz frequency observations of GWs produced during inflation. Finally, we examined the impact of the e-fold number in our numerical analysis by taking into account the lower bound of $N_e = 50$ as considered by Planck. In this case, we found no substantial discrepancies with respect to the results obtained by assuming the concordance value of $N_e = 60$.

Future perspectives of our work include extending the current analysis to different functional forms of the dissipation coefficient, such as $\Gamma \propto T^3$, and exploring alternative inflationary potentials. Moreover, further insights into warm inflation could be inferred by investigating whether the present results are confirmed in the strong dissipation regime, i.e., for $Q \gg 1$.

ACKNOWLEDGMENTS

The authors would like to thank the Reviewer for all helpful and constructive comments on the manuscript. The authors acknowledge the financial support of the Istituto Nazionale di Fisica Nucleare (INFN) - Sezione di Napoli, *iniziative specifiche* QGSKY and MOONLIGHT. R.D. acknowledges work from COST Action CA21136 - Addressing observational tensions in cosmology with systematics and fundamental physics (CosmoVerse).

-
- [1] A. A. Starobinsky, A New Type of Isotropic Cosmological Models Without Singularity, *Phys. Lett. B* **91**, 99 (1980).
 - [2] A. H. Guth, The Inflationary Universe: A Possible Solution to the Horizon and Flatness Problems, *Phys. Rev. D* **23**, 347 (1981).
 - [3] A. D. Linde, A New Inflationary Universe Scenario: A Possible Solution of the Horizon, Flatness, Homogeneity, Isotropy and Primordial Monopole Problems, *Phys. Lett. B* **108**, 389 (1982).
 - [4] A. Albrecht and P. J. Steinhardt, Cosmology for Grand Unified Theories with Radiatively Induced Symmetry Breaking, *Phys. Rev. Lett.* **48**, 1220 (1982).
 - [5] A. Albrecht, P. J. Steinhardt, M. S. Turner, and F. Wilczek, Reheating an Inflationary Universe, *Phys. Rev. Lett.* **48**, 1437 (1982).
 - [6] L. F. Abbott, E. Farhi, and M. B. Wise, Particle Production in the New Inflationary Cosmology, *Phys. Lett. B* **117**, 29 (1982).
 - [7] R. D'Agostino, O. Luongo, and M. Muccino, Healing the cosmological constant problem during inflation through a unified quasi-quintessence matter field, *Class. Quant. Grav.* **39**, 195014 (2022), arXiv:2204.02190 [gr-qc].
 - [8] A. Berera and L.-Z. Fang, Thermally induced density perturbations in the inflation era, *Phys. Rev. Lett.* **74**, 1912 (1995), arXiv:astro-ph/9501024.

- [9] A. Berera, Warm inflation, *Phys. Rev. Lett.* **75**, 3218 (1995), [arXiv:astro-ph/9509049](#).
- [10] A. Berera, M. Gleiser, and R. O. Ramos, A First principles warm inflation model that solves the cosmological horizon / flatness problems, *Phys. Rev. Lett.* **83**, 264 (1999), [arXiv:hep-ph/9809583](#).
- [11] L. Visinelli, Observational Constraints on Monomial Warm Inflation, *JCAP* **07**, 054, [arXiv:1605.06449 \[astro-ph.CO\]](#).
- [12] M. Benetti and R. O. Ramos, Warm inflation dissipative effects: predictions and constraints from the Planck data, *Phys. Rev. D* **95**, 023517 (2017), [arXiv:1610.08758 \[astro-ph.CO\]](#).
- [13] S. Das and R. O. Ramos, Graceful exit problem in warm inflation, *Phys. Rev. D* **103**, 123520 (2021), [arXiv:2005.01122 \[gr-qc\]](#).
- [14] R. D'Agostino and O. Luongo, Cosmological viability of a double field unified model from warm inflation, *Phys. Lett. B* **829**, 137070 (2022), [arXiv:2112.12816 \[astro-ph.CO\]](#).
- [15] A. Berera, I. G. Moss, and R. O. Ramos, Warm Inflation and its Microphysical Basis, *Rept. Prog. Phys.* **72**, 026901 (2009), [arXiv:0808.1855 \[hep-ph\]](#).
- [16] A. Berera, Thermal properties of an inflationary universe, *Phys. Rev. D* **54**, 2519 (1996), [arXiv:hep-th/9601134](#).
- [17] A. Berera, M. Gleiser, and R. O. Ramos, Strong dissipative behavior in quantum field theory, *Phys. Rev. D* **58**, 123508 (1998), [arXiv:hep-ph/9803394](#).
- [18] A. Berera, Warm inflation at arbitrary adiabaticity: A Model, an existence proof for inflationary dynamics in quantum field theory, *Nucl. Phys. B* **585**, 666 (2000), [arXiv:hep-ph/9904409](#).
- [19] A. Berera and R. O. Ramos, Construction of a robust warm inflation mechanism, *Phys. Lett. B* **567**, 294 (2003), [arXiv:hep-ph/0210301](#).
- [20] M. Bastero-Gil, A. Berera, R. O. Ramos, and J. G. Rosa, Warm Little Inflaton, *Phys. Rev. Lett.* **117**, 151301 (2016), [arXiv:1604.08838 \[hep-ph\]](#).
- [21] K. V. Berghaus, P. W. Graham, and D. E. Kaplan, Minimal Warm Inflation, *JCAP* **03**, 034, [Erratum: *JCAP* **10**, E02 (2023)], [arXiv:1910.07525 \[hep-ph\]](#).
- [22] M. Bastero-Gil, A. Berera, R. O. Ramos, and J. a. G. Rosa, Towards a reliable effective field theory of inflation, *Phys. Lett. B* **813**, 136055 (2021), [arXiv:1907.13410 \[hep-ph\]](#).
- [23] M. Motaharf, V. Kamali, and R. O. Ramos, Warm inflation as a way out of the swampland, *Phys. Rev. D* **99**, 063513 (2019), [arXiv:1810.02816 \[astro-ph.CO\]](#).
- [24] S. Das, Warm Inflation in the light of Swampland Criteria, *Phys. Rev. D* **99**, 063514 (2019), [arXiv:1810.05038 \[hep-th\]](#).
- [25] A. Berera and J. R. Calderón, Trans-Planckian censorship and other swampland bothers addressed in warm inflation, *Phys. Rev. D* **100**, 123530 (2019), [arXiv:1910.10516 \[hep-ph\]](#).
- [26] I. G. Moss, Primordial Inflation With Spontaneous Symmetry Breaking, *Phys. Lett. B* **154**, 120 (1985).
- [27] H. P. De Oliveira and S. E. Joras, On perturbations in warm inflation, *Phys. Rev. D* **64**, 063513 (2001), [arXiv:gr-qc/0103089](#).
- [28] K. Dimopoulos and L. Donaldson-Wood, Warm quintessential inflation, *Phys. Lett. B* **796**, 26 (2019), [arXiv:1906.09648 \[gr-qc\]](#).
- [29] V. Kamali, M. Motaharf, and R. O. Ramos, Recent Developments in Warm Inflation, *Universe* **9**, 124 (2023), [arXiv:2302.02827 \[hep-ph\]](#).
- [30] G. Ballesteros, A. Perez Rodriguez, and M. Pierre, Monomial warm inflation revisited, *JCAP* **03**, 003, [arXiv:2304.05978 \[astro-ph.CO\]](#).
- [31] S. Bird, I. Cholis, J. B. Muñoz, Y. Ali-Haïmoud, M. Kamionkowski, E. D. Kovetz, A. Raccanelli, and A. G. Riess, Did LIGO detect dark matter?, *Phys. Rev. Lett.* **116**, 201301 (2016), [arXiv:1603.00464 \[astro-ph.CO\]](#).
- [32] B. P. Abbott *et al.* (LIGO Scientific, Virgo, 1M2H, Dark Energy Camera GW-E, DES, DLT40, Las Cumbres Observatory, VINROUGE, MASTER), A gravitational-wave standard siren measurement of the Hubble constant, *Nature* **551**, 85 (2017), [arXiv:1710.05835 \[astro-ph.CO\]](#).
- [33] J. M. Ezquiaga and M. Zumalacárregui, Dark Energy After GW170817: Dead Ends and the Road Ahead, *Phys. Rev. Lett.* **119**, 251304 (2017), [arXiv:1710.05901 \[astro-ph.CO\]](#).
- [34] E. Belgacem, Y. Dirian, S. Foffa, and M. Maggiore, Gravitational-wave luminosity distance in modified gravity theories, *Phys. Rev. D* **97**, 104066 (2018), [arXiv:1712.08108 \[astro-ph.CO\]](#).
- [35] R. D'Agostino and R. C. Nunes, Probing observational bounds on scalar-tensor theories from standard sirens, *Phys. Rev. D* **100**, 044041 (2019), [arXiv:1907.05516 \[gr-qc\]](#).
- [36] A. Bonilla, R. D'Agostino, R. C. Nunes, and J. C. N. de Araujo, Forecasts on the speed of gravitational waves at high z , *JCAP* **03**, 015, [arXiv:1910.05631 \[gr-qc\]](#).
- [37] K. G. Arun *et al.* (LISA), New horizons for fundamental physics with LISA, *Living Rev. Rel.* **25**, 4 (2022), [arXiv:2205.01597 \[gr-qc\]](#).
- [38] R. D'Agostino and R. C. Nunes, Forecasting constraints on deviations from general relativity in $f(Q)$ gravity with standard sirens, *Phys. Rev. D* **106**, 124053 (2022), [arXiv:2210.11935 \[gr-qc\]](#).
- [39] R. D'Agostino, M. Califano, N. Menadeo, and D. Vernieri, Role of spatial curvature in the primordial gravitational wave power spectrum, *Phys. Rev. D* **108**, 043538 (2023), [arXiv:2305.14238 \[astro-ph.CO\]](#).
- [40] P. Athron, C. Balázs, A. Fowlie, L. Morris, and L. Wu, Cosmological phase transitions: From perturbative particle physics to gravitational waves, *Prog. Part. Nucl. Phys.* **135**, 104094 (2024), [arXiv:2305.02357 \[hep-ph\]](#).
- [41] M. Califano, R. D'Agostino, and D. Vernieri, Parity violation in gravitational waves and observational bounds from third-generation detectors, (2023), [arXiv:2311.02161 \[gr-qc\]](#).
- [42] K. Tomita, Non-Linear Theory of Gravitational Instability in the Expanding Universe, *Prog. Theor. Phys.* **37**, 831 (1967).
- [43] S. Matarrese, O. Pantano, and D. Saez, General relativistic dynamics of irrotational dust: Cosmological implications, *Phys. Rev. Lett.* **72**, 320 (1994), [arXiv:astro-ph/9310036](#).
- [44] S. Matarrese, S. Mollerach, and M. Bruni, Second order perturbations of the Einstein-de Sitter universe, *Phys. Rev. D* **58**, 043504 (1998), [arXiv:astro-ph/9707278](#).
- [45] G. Domènech, Scalar Induced Gravitational Waves Review, *Universe* **7**, 398 (2021), [arXiv:2109.01398 \[gr-qc\]](#).
- [46] A. Afzal *et al.* (NANOGrav), The NANOGrav 15 yr Data Set: Search for Signals from New Physics, *Astrophys. J.*

- Lett.* **951**, L11 (2023), [arXiv:2306.16219 \[astro-ph.HE\]](#).
- [47] G. Agazie *et al.* (NANOGrav), The NANOGrav 15 yr Data Set: Evidence for a Gravitational-wave Background, *Astrophys. J. Lett.* **951**, L8 (2023), [arXiv:2306.16213 \[astro-ph.HE\]](#).
- [48] J. Antoniadis *et al.* (EPTA, InPTA:), The second data release from the European Pulsar Timing Array - III. Search for gravitational wave signals, *Astron. Astrophys.* **678**, A50 (2023), [arXiv:2306.16214 \[astro-ph.HE\]](#).
- [49] J. Antoniadis *et al.* (EPTA), The second data release from the European Pulsar Timing Array: V. Implications for massive black holes, dark matter and the early Universe, (2023), [arXiv:2306.16227 \[astro-ph.CO\]](#).
- [50] J. Antoniadis *et al.* (EPTA), The second data release from the European Pulsar Timing Array - I. The dataset and timing analysis, *Astron. Astrophys.* **678**, A48 (2023), [arXiv:2306.16224 \[astro-ph.HE\]](#).
- [51] M. Califano, R. D'Agostino, and D. Vernieri, Can the NANOGrav observations constrain the geometry of the Universe?, *Phys. Rev. D* **109**, 083520 (2024), [arXiv:2403.15373 \[astro-ph.CO\]](#).
- [52] M. Bastero-Gil and A. Berera, Warm inflation model building, *Int. J. Mod. Phys. A* **24**, 2207 (2009), [arXiv:0902.0521 \[hep-ph\]](#).
- [53] L. M. H. Hall, I. G. Moss, and A. Berera, Scalar perturbation spectra from warm inflation, *Phys. Rev. D* **69**, 083525 (2004), [arXiv:astro-ph/0305015](#).
- [54] S. Bartrum, M. Bastero-Gil, A. Berera, R. Cerezo, R. O. Ramos, and J. G. Rosa, The importance of being warm (during inflation), *Phys. Lett. B* **732**, 116 (2014), [arXiv:1307.5868 \[hep-ph\]](#).
- [55] M. Bastero-Gil, A. Berera, and R. O. Ramos, Shear viscous effects on the primordial power spectrum from warm inflation, *JCAP* **07**, 030, [arXiv:1106.0701 \[astro-ph.CO\]](#).
- [56] K. N. Ananda, C. Clarkson, and D. Wands, The Cosmological gravitational wave background from primordial density perturbations, *Phys. Rev. D* **75**, 123518 (2007), [arXiv:gr-qc/0612013](#).
- [57] V. Mukhanov, *Physical Foundations of Cosmology* (Cambridge University Press, Oxford, 2005).
- [58] D. Baumann, P. J. Steinhardt, K. Takahashi, and K. Ichiki, Gravitational Wave Spectrum Induced by Primordial Scalar Perturbations, *Phys. Rev. D* **76**, 084019 (2007), [arXiv:hep-th/0703290](#).
- [59] K. Kohri and T. Terada, Semianalytic calculation of gravitational wave spectrum nonlinearly induced from primordial curvature perturbations, *Phys. Rev. D* **97**, 123532 (2018), [arXiv:1804.08577 \[gr-qc\]](#).
- [60] J. R. Espinosa, D. Racco, and A. Riotto, A Cosmological Signature of the SM Higgs Instability: Gravitational Waves, *JCAP* **09**, 012, [arXiv:1804.07732 \[hep-ph\]](#).
- [61] K. Saikawa and S. Shirai, Precise WIMP Dark Matter Abundance and Standard Model Thermodynamics, *JCAP* **08**, 011, [arXiv:2005.03544 \[hep-ph\]](#).
- [62] N. Aghanim *et al.* (Planck), Planck 2018 results. VI. Cosmological parameters, *Astron. Astrophys.* **641**, A6 (2020), [Erratum: *Astron. Astrophys.* 652, C4 (2021)], [arXiv:1807.06209 \[astro-ph.CO\]](#).
- [63] A. D. Linde, Chaotic Inflation, *Phys. Lett. B* **129**, 177 (1983).
- [64] M. Kawasaki, M. Yamaguchi, and T. Yanagida, Natural chaotic inflation in supergravity, *Phys. Rev. Lett.* **85**, 3572 (2000), [arXiv:hep-ph/0004243](#).
- [65] C.-Q. Geng, M. W. Hossain, R. Myrzakulov, M. Sami, and E. N. Saridakis, Quintessential inflation with canonical and noncanonical scalar fields and Planck 2015 results, *Phys. Rev. D* **92**, 023522 (2015), [arXiv:1502.03597 \[gr-qc\]](#).
- [66] G. B. F. Lima and R. O. Ramos, Unified early and late Universe cosmology through dissipative effects in steep quintessential inflation potential models, *Phys. Rev. D* **100**, 123529 (2019), [arXiv:1910.05185 \[astro-ph.CO\]](#).
- [67] S. Das and R. O. Ramos, Runaway potentials in warm inflation satisfying the swampland conjectures, *Phys. Rev. D* **102**, 103522 (2020), [arXiv:2007.15268 \[hep-th\]](#).
- [68] S. Das, G. Goswami, and C. Krishnan, Swampland, axions, and minimal warm inflation, *Phys. Rev. D* **101**, 103529 (2020), [arXiv:1911.00323 \[hep-th\]](#).
- [69] G. Agazie *et al.* (NANOGrav), The NANOGrav 15 yr Data Set: Observations and Timing of 68 Millisecond Pulsars, *Astrophys. J. Lett.* **951**, L9 (2023), [arXiv:2306.16217 \[astro-ph.HE\]](#).
- [70] W. G. Lamb, S. R. Taylor, and R. van Haasteren, Rapid refitting techniques for Bayesian spectral characterization of the gravitational wave background using pulsar timing arrays, *Phys. Rev. D* **108**, 103019 (2023), [arXiv:2303.15442 \[astro-ph.HE\]](#).
- [71] A. Mitridate, D. Wright, R. von Eckardstein, T. Schröder, J. Nay, K. Olum, K. Schmitz, and T. Trickle, PTArcade, (2023), [arXiv:2306.16377 \[hep-ph\]](#).
- [72] J. Ellis and R. Van Haasteren, [jellis18/PTMCMCSampler: Official Release](#) (2017).
- [73] F. C. Adams, K. Freese, and A. H. Guth, Constraints on the scalar field potential in inflationary models, *Phys. Rev. D* **43**, 965 (1991).
- [74] R. Trotta, Bayes in the sky: Bayesian inference and model selection in cosmology, *Contemp. Phys.* **49**, 71 (2008), [arXiv:0803.4089 \[astro-ph\]](#).
- [75] H. Jeffreys, *The Theory of Probability*, Oxford Classic Texts in the Physical Sciences (1939).
- [76] Y. Akrami *et al.* (Planck), Planck 2018 results. X. Constraints on inflation, *Astron. Astrophys.* **641**, A10 (2020), [arXiv:1807.06211 \[astro-ph.CO\]](#).
- [77] M. C. Guzzetti, N. Bartolo, M. Liguori, and S. Matarrese, Gravitational waves from inflation, *Riv. Nuovo Cim.* **39**, 399 (2016), [arXiv:1605.01615 \[astro-ph.CO\]](#).